

# Mechanism of C–P Reductive Elimination from *trans*-[Pd(CH=CHPh)Br(PMePh<sub>2</sub>)<sub>2</sub>]

Masayuki Wakioka, Yumiko Nakajima, and Fumiyuki Ozawa\*

International Research Center for Elements Science (IRCELS), Institute for Chemical Research, Kyoto University, Uji, Kyoto 611-0011, Japan

Received December 20, 2008

The (*E*)- and (*Z*)-styryl isomers of *trans*-[Pd(CH=CHPh)Br(PMePh<sub>2</sub>)<sub>2</sub>] (**1a**) and [Pd( $\eta^2$ -PhCH=CHPMePh<sub>2</sub>)Br(PMePh<sub>2</sub>)<sub>2</sub>] (**2a**) were prepared, and their C–P reductive elimination (**1a** → **2a**) and C–P oxidative addition (**2a** → **1a**) behaviors examined. Kinetics and thermodynamics of the reactions are strongly affected by *E/Z* configurations of the styryl group and solvent polarity. Complex (*E*)-**1a** readily undergoes C–P reductive elimination in CD<sub>2</sub>Cl<sub>2</sub> as a polar solvent in high selectivity. On the other hand, while the (*Z*)-isomer of **1a** is unreactive toward reductive elimination, (*Z*)-**2a** undergoes C–P oxidative addition favorably in nonpolar benzene. X-ray diffraction analysis and DFT calculations for **1a** and **2a** provided reasonable accounts for these reaction features. Kinetic examinations revealed two types of C–P reductive elimination processes, which involve predissociation and association of the PMePh<sub>2</sub> ligand, respectively.

## Introduction

Reductive elimination is a crucial elementary process, often serving as the product-forming step in many catalytic organic transformations.<sup>1</sup> Besides classical reactions to afford C–H and C–C bonds, reductive elimination of a carbon–heteroatom bond has attracted considerable recent attention in connection with palladium-catalyzed synthesis of heteroatom compounds.<sup>2</sup> While the C–N and C–O bond formations are of central importance in such chemistry, there has been a growing interest in C–P reductive elimination of hydrocarbyl and phosphine ligands from Pd(II) complexes.<sup>3–7</sup> It has been documented that complexes of the formula [PdAr(X)(PAr')<sub>2</sub>] (Ar, Ar' = aryl; X = halogen) undergo C–P reductive elimination to give arylphosphonium halides (PArAr'<sub>3</sub>·X) and Pd(0) species.<sup>3</sup> This reaction is usually reversible with C–P oxidative addition, and the overall process

results in Ar/Ar' exchange between palladium and phosphorus atoms.<sup>8</sup> The C–P reductive elimination has also been postulated for catalytic formation of aryl-,<sup>4</sup> alkenyl-,<sup>5</sup> and alkyl-phosphoniums<sup>6</sup> and functionalized phosphines.<sup>7</sup>

Most of the reductive elimination processes involve the coupling of two anionic ligands. In contrast, C–P reductive elimination causes the bond formation between anionic and

\* To whom correspondence should be addressed. E-mail: ozawa@scl.kyoto-u.ac.jp.

(1) (a) Ozawa, F. In *Current Methods in Inorganic Chemistry Volume 3, Fundamentals of Molecular Catalysis*; Yamamoto, A., Kurosawa, H., Eds.; Elsevier Science: Amsterdam, The Netherlands, 2003; Chapter 9. (b) Crabtree, R. H. *The Organometallic Chemistry of the Transition Metals*, 4th ed.; John Wiley & Sons: Hoboken, NJ, 2005; pp 55–60. (c) Yamamoto, A. *Organotransition Metal Chemistry, Fundamental Concepts and Application*; John Wiley & Sons: New York, NY, 1986; pp 240–245. (d) Collman, J. P.; Hegedus, L. S.; Norton, J. R.; Finke, R. G. *Principles and Applications of Organotransition Metal Chemistry*; University Science Books: Mill Valley, CA, 1987; pp 323–353. (e) Brown, J. M.; Cooley, N. A. *Chem. Rev.* **1988**, *88*, 1031–1046.

(2) (a) Muci, A. R.; Buchwald, S. L. *Top. Curr. Chem.* **2002**, *219*, 131–209. (b) Hartwig, J. F. *Inorg. Chem.* **2007**, *46*, 1936–1947. (c) Hartwig, J. F. *Nature* **2008**, *455*, 314–322.

(3) (a) Kong, K.-C.; Cheng, C.-H. *J. Am. Chem. Soc.* **1991**, *113*, 6313–6315. (b) Goodson, F. E.; Wallow, T. I.; Novak, B. M. *J. Am. Chem. Soc.* **1997**, *119*, 12441–12453. (c) Grushin, V. V. *Organometallics* **2000**, *19*, 1888–1900. (d) Herrmann, W. A.; Brossmer, C.; Priermeier, T.; Oefele, K. *J. Organomet. Chem.* **1994**, *481*, 97–108. (e) Segelstein, B. E.; Bulter, T. W.; Chenard, B. L. *J. Org. Chem.* **1995**, *60*, 12–13. (f) Sakamoto, M.; Shimizu, I.; Yamamoto, A. *Chem. Lett.* **1995**, 1101–1102. (g) Vicente, J.; Abad, J.-A.; Martinez-Viviente, E.; Ramirez de Arellano, M. C.; Jones, P. G. *Organometallics* **2000**, *19*, 752–760. (h) Marshall, W. J.; Grushin, V. V. *Organometallics* **2003**, *22*, 555–562. (i) Hwang, L. K.; Na, Y.; Lee, J.; Do, Y.; Chang, S. *Angew. Chem., Int. Ed.* **2005**, *44*, 6166–6169. (j) Macgregor, S. A. *Chem. Soc. Rev.* **2007**, *36*, 67–76.

(4) (a) Migita, T.; Shimizu, T.; Asami, Y.; Shiobara, J.; Kato, Y.; Kosugi, M. *Bull. Chem. Soc. Jpn.* **1980**, *53*, 1385–1389. (b) Migita, T.; Nagai, T.; Kiuchi, K.; Kosugi, M. *Bull. Chem. Soc. Jpn.* **1983**, *56*, 2869–2870. (c) Clark, J. H.; Tavener, S. J.; Barlow, S. J. *J. Mater. Chem.* **1995**, *5*, 827–830. (d) Vicente, J.; Abad, J.-A.; Frankland, A. D.; De Arellano, M. C. R. *Chem.–Eur. J.* **1999**, *5*, 3066–3075. (e) Bourgogne, C.; Le, F. Y.; Juen, P.; Masson, P.; Nicoud, J.-F.; Masse, R. *Chem. Mater.* **2000**, *12*, 1025–1033. (f) Lambert, C.; Gaschler, W.; Noll, G.; Weber, M.; Schmalzlin, E.; Brauchle, C.; Meerholz, K. *J. Chem. Soc., Perkin Trans. 2* **2001**, *6*, 964–974. (g) de la Torre, G.; Gouloumis, A.; Vazquez, P.; Torres, T. *Angew. Chem., Int. Ed.* **2001**, *40*, 2895–2898. (h) Cheng, Z.; Subbarayan, M.; Chen, X.; Gambhir, S. S. *J. Label. Compd. Radiopharm.* **2005**, *48*, 131–137. (i) Marcoux, D.; Charette, A. B. *J. Org. Chem.* **2008**, *73*, 590–593.

(5) (a) Huang, C.-C.; Duan, J.-P.; Wu, M.-Y.; Liao, F.-L.; Wang, S.-L.; Cheng, C.-H. *Organometallics* **1998**, *17*, 676–682. (b) Rybin, L. V.; Petrovskaya, E. A.; Rubinskaya, M. I.; Kuz'mina, L. G.; Struchkov, Y. T.; Kaverin, V. V.; Koneva, N. Y. *J. Organomet. Chem.* **1985**, *288*, 119–129. (c) Kowalski, M. H.; Hinkle, R. J.; Stang, P. J. *J. Org. Chem.* **1989**, *54*, 2783–2784. (d) Hinkle, R. J.; Stang, P. J.; Kowalski, M. H. *J. Org. Chem.* **1990**, *55*, 5033–5036. (e) Dervisi, A.; Edwards, P. G.; Newman, P. D.; Tooze, R. P. *Dalton* **2000**, 523–528. (f) Arisawa, M.; Yamaguchi, M. *J. Am. Chem. Soc.* **2000**, *122*, 2387–2388. (g) Jutand, A.; Negri, S. *Organometallics* **2003**, *22*, 4229–4237.

(6) (a) Arisawa, M.; Yamaguchi, M. *J. Am. Chem. Soc.* **2006**, *128*, 50–51. (b) Arisawa, M.; Yamaguchi, M. *Adv. Synth. Catal.* **2001**, *343*, 27–28.

(7) (a) Kwong, F. Y.; Chan, K. S. *Organometallics* **2000**, *19*, 2058–2060. (b) Kwong, F. Y.; Chan, K. S. *Chem. Commun.* **2000**, 1069–1070. (c) Kwong, F. Y.; Lai, C. W.; Tian, Y.; Chan, K. S. *Tetrahedron Lett.* **2000**, *41*, 10285–10289. (d) Kwong, F. Y.; Chan, K. S. *Organometallics* **2001**, *20*, 2570–2578. (e) Lai, C. W.; Kwong, F. Y.; Wang, Y.; Chan, K. S. *Tetrahedron Lett.* **2001**, *42*, 4883–4885. (f) Kwong, F. Y.; Lai, C. W.; Chan, K. S. *Tetrahedron Lett.* **2002**, *43*, 3537–3539. (g) Kwong, F. Y.; Lai, C. W.; Yu, M.; Tian, Y.; Chan, K. S. *Tetrahedron* **2003**, *59*, 10295–10305. (h) Kwong, F. Y.; Lai, C. W.; Yu, M.; Chan, K. S. *Tetrahedron* **2004**, *60*, 5635–5645. (i) Wang, Y.; Lai, C. W.; Kwong, F. Y.; Jia, W.; Chan, K. S. *Tetrahedron* **2004**, *60*, 9433–9439.

(8) An alternative mechanism involving a phosphido intermediate has been proposed for the conversion of *trans*-[PdMe(I)(PPh<sub>3</sub>)<sub>2</sub>] to [PdPh(I)-(PMePh<sub>2</sub>)(PPh<sub>3</sub>)]: Morita, D. K.; Stille, J. K.; Norton, J. R. *J. Am. Chem. Soc.* **1995**, *117*, 8576–8581.

**Table 1.** C–P Reductive Elimination of *trans*-[Pd{CH=CHPh-(*E*)}Br(PR<sub>3</sub>)<sub>2</sub>] ((*E*)-**1**)<sup>a</sup>

run	complex	solvent	additive (PR <sub>3</sub> , mM)	temp (°C)	<i>t</i> <sub>1/2</sub> <sup>b</sup> (min)	selectivity of <b>2</b> (or <b>3</b> ) (%)
1	( <i>E</i> )- <b>1a</b>	CD <sub>2</sub> Cl <sub>2</sub>	0	40	ca. 5	82
2	( <i>E</i> )- <b>1a</b>	CD <sub>2</sub> Cl <sub>2</sub>	50	40	168	97 <sup>c</sup>
3	( <i>E</i> )- <b>1a</b>	THF- <i>d</i> <sub>8</sub>	0	50	48	67
4	( <i>E</i> )- <b>1a</b>	C <sub>6</sub> D <sub>6</sub>	0	50	60	56
5	( <i>E</i> )- <b>1b</b>	CD <sub>2</sub> Cl <sub>2</sub>	0	40	<4	63
6	( <i>E</i> )- <b>1b</b>	CD <sub>2</sub> Cl <sub>2</sub>	50	40	35	96 <sup>d</sup>
7	( <i>E</i> )- <b>1c</b>	CD <sub>2</sub> Cl <sub>2</sub>	0	40	270	43 <sup>e</sup>

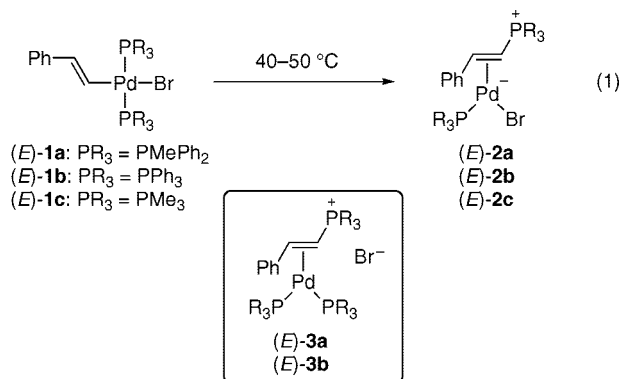
<sup>a</sup> [I]<sub>0</sub> = 50 mM. All reactions were examined by <sup>1</sup>H NMR spectroscopy using 1,3,5-trimethoxybenzene as an internal standard. <sup>b</sup> Half-lives of **1**. <sup>c</sup> The sum of [Pd{η<sup>2</sup>-(*E*)-PhCH=CHPMePh<sub>2</sub>}(PMePh<sub>2</sub>)<sub>2</sub>]Br ((*E*)-**3a**) (96%) and (*E*)-PhCH=CHPMePh<sub>2</sub>·Br (1%). <sup>d</sup> The product was [Pd{η<sup>2</sup>-(*E*)-PhCH=CHPPh<sub>3</sub>}(PPh<sub>3</sub>)<sub>2</sub>]Br ((*E*)-**3b**). <sup>e</sup> The selectivity at 58% conversion of (*E*)-**1c**.

neutral ligands. Accordingly, it is expected that the reaction possesses rather unique mechanistic features, differing significantly from common reductive elimination processes. Although the reductive elimination of arylphosphonium from [PdAr(X)-(PAR'<sub>3</sub>)<sub>2</sub>]-type complexes has been suggested to involve prior dissociation of one of the phosphine ligands,<sup>3a–c</sup> intimate information about the mechanism of C–P reductive elimination is still limited.<sup>9</sup> This is probably due to the concurrent operation of C–P oxidative addition, which makes the reaction system complicated.

This paper deals with C–P reductive elimination from *trans*-[Pd(CH=CHPh)Br(PMePh<sub>2</sub>)<sub>2</sub>] (**1a**) to afford [Pd(η<sup>2</sup>-PhCH=CHPMePh<sub>2</sub>)Br(PMePh<sub>2</sub>)<sub>2</sub>] (**2a**) and [Pd(η<sup>2</sup>-PhCH=CHPMePh<sub>2</sub>)-(PMePh<sub>2</sub>)<sub>2</sub>]Br (**3a**). Unlike the reactions of arylpalladium complexes,<sup>3</sup> the C–P reductive elimination of styryl complexes forms η<sup>2</sup>-styrylphosphonium complexes as the products, which are sufficiently stable for isolation.<sup>10</sup> Therefore, we anticipated that the reaction is capable of mechanistic investigations using kinetic techniques. We herein describe that C–P reductive elimination of **1a** is strongly dependent on *E/Z* configurations of the styryl ligand. It has also been found that two types of reductive elimination processes are operative, depending on the amount of free PMePh<sub>2</sub> in the system.

## Results and Discussion

**C–P Reductive Elimination and Oxidative Addition Reactions.** (*E*)-Styryl complexes having three kinds of tertiary phosphine ligands ((*E*)-**1a–c**) were heated in solution, and the reaction systems were examined at intervals by <sup>1</sup>H NMR spectroscopy (eq 1). The results are summarized in Table 1.



Complex (*E*)-**1a**, bearing PMePh<sub>2</sub> ligands, readily underwent C–P reductive elimination in CD<sub>2</sub>Cl<sub>2</sub> at 40 °C to give the corresponding styrylphosphonium complex ((*E*)-**2a**) in 82%

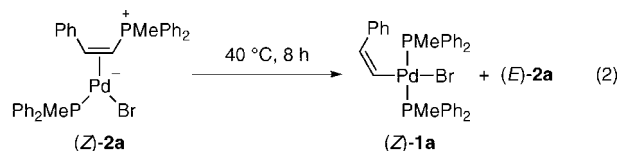
**Table 2.** C–P Oxidative Addition of [Pd{η<sup>2</sup>-(*Z*)-PhCH=CHPMePh<sub>2</sub>}Br(PMePh<sub>2</sub>)<sub>2</sub>] ((*Z*)-**2a**)<sup>a</sup>

run	solvent	PMePh <sub>2</sub> (mM)	conversion of ( <i>Z</i> )- <b>2a</b> (%)	selectivity (%)	
				( <i>Z</i> )- <b>1a</b>	( <i>E</i> )- <b>2a</b>
1	C <sub>6</sub> D <sub>6</sub>	0	79	46	33
2	C <sub>6</sub> D <sub>6</sub>	10	90	0	100
3	CD <sub>2</sub> Cl <sub>2</sub>	0	27	12	73

<sup>a</sup> [(*Z*)-**2a**]<sub>0</sub> = 10 mM. All reactions were run at 40 °C for 8 h.

selectivity (run 1). The remaining part of (*E*)-**1a** was converted to *trans*-[PdBr<sub>2</sub>(PMePh<sub>2</sub>)<sub>2</sub>] (5%) and some unidentified palladium species. We already confirmed that the dibromo complex is afforded by disproportionation of (*E*)-**1a**, and its formation is inhibited by free PMePh<sub>2</sub>.<sup>11</sup> Actually, in the presence of added PMePh<sub>2</sub> (1 equiv/**1a**), the C–P reductive elimination proceeded in 97% selectivity (run 2), where the product styrylphosphonium complex was obtained as [Pd{η<sup>2</sup>-(*E*)-PhCH=CHPMePh<sub>2</sub>}(PMePh<sub>2</sub>)<sub>2</sub>]Br ((*E*)-**3a**), instead of (*E*)-**2a**.<sup>12</sup> The conversion of (*E*)-**1a** was strongly affected by solvent polarity; the reaction decelerated significantly in THF and benzene, and the selectivity of (*E*)-**2a** decreased (runs 3 and 4). The PPh<sub>3</sub> complex (*E*)-**1b** behaved similarly, while the reactivity was apparently higher than that of (*E*)-**1a** (runs 5 and 6). On the other hand, the PMe<sub>3</sub> complex (*E*)-**1c** was much less reactive than (*E*)-**1a** and (*E*)-**1b** (run 7).

Unlike the (*E*)-styryl complexes, the (*Z*)-isomer *trans*-[Pd{CH=CHPh-(*Z*)}Br(PMePh<sub>2</sub>)<sub>2</sub>] ((*Z*)-**1a**) was stable toward C–P reductive elimination; no trace of [Pd{η<sup>2</sup>-(*Z*)-PhCH=CHPMePh<sub>2</sub>}Br(PMePh<sub>2</sub>)<sub>2</sub>] ((*Z*)-**2a**) was formed at 50 °C for 6 h. On the contrary, (*Z*)-**2a** was found to undergo oxidative addition of styrylphosphonium ligand (eq 2, Table 2). Heating a C<sub>6</sub>D<sub>6</sub> solution of isolated (*Z*)-**2a** at 40 °C for 8 h resulted in the formation of (*Z*)-**1a** in 46% selectivity, together with (*E*)-**2a** (33%) and other palladium complexes including *trans*-[PdBr<sub>2</sub>(PMePh<sub>2</sub>)<sub>2</sub>] (4%) (run 1). The formation of (*Z*)-**1a** was entirely suppressed by added PMePh<sub>2</sub> (1 equiv/**1a**), while the *Z*-to-*E* isomerization of the styrylphosphonium ligand giving (*E*)-**2a** continued to proceed at a comparable rate (run 2). The reaction rate and the selectivity of (*Z*)-**1a** decreased significantly in CD<sub>2</sub>Cl<sub>2</sub> as a polar solvent (run 3).



**X-ray Structures of **1a** and **2a**.** It has been found that reductive elimination and oxidative addition reactions of C–P bonds are markedly affected by *E/Z* configurations of the styryl group and solvent polarity. Since these reactions are essentially reverse processes, and the conversion of (*E*)-**1a** to (*E*)-**2a** and

(9) The mechanism of C–P reductive elimination of anionic phosphorus ligands such as phosphido and phosphonato has been examined using isolated complexes: (a) Gaumont, A.-C.; Brown, J. M.; Hursthouse, M. B.; Coles, S. J. *Chem. Commun.* **1999**, 63–64. (b) Adam, M.; Stockland, R. A., Jr.; Clark, R.; Guzei, I. *Organometallics* **2002**, *21*, 3278–3284. (c) Stockland, R. A., Jr.; Levine, A. M.; Giovine, M. T.; Guzei, I. A.; Cannistra, J. C. *Organometallics* **2004**, *23*, 647–656. (d) Kohler, M. C.; Stockland, R. A., Jr.; Rath, N. P. *Organometallics* **2006**, *25*, 5746–5756. (e) Kalek, M.; Stawinski, J. *Organometallics* **2008**, *27*, 5876–5888.

(10) The C–P reductive elimination of a styryl complex has been reported for *trans*-[Pd{CH=CHPh-(*E*)}Br(PPh<sub>3</sub>)<sub>2</sub>] (**1b**).<sup>5a</sup>

(11) Wakioka, M.; Nagao, M.; Ozawa, F. *Organometallics* **2008**, *27*, 602–608.

(12) The PPh<sub>3</sub> analogue [Pd{η<sup>2</sup>-(*E*)-PhCH=CHPPh<sub>3</sub>}(PPh<sub>3</sub>)<sub>2</sub>]Br ((*E*)-**3b**) has been reported.<sup>5a</sup>

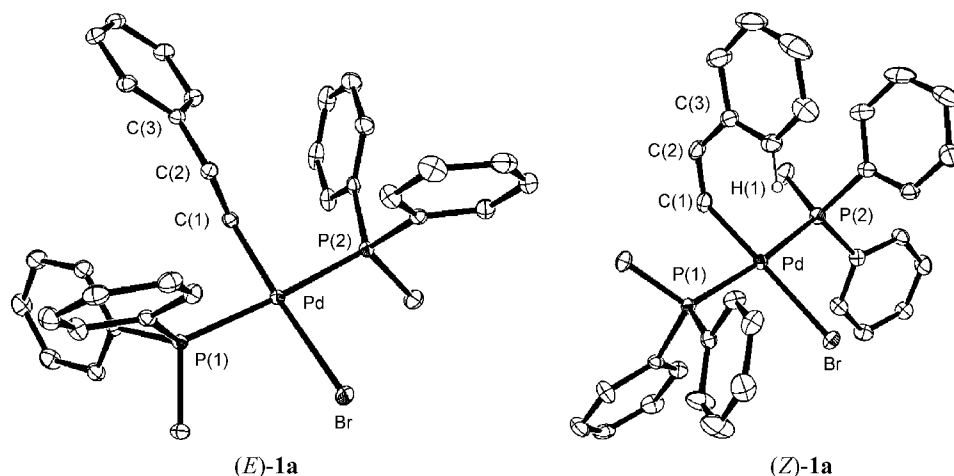


**Figure 1.** X-ray structures of (*E*)-**1a** and (*Z*)-**1a** (one of the crystallographically independent molecules). Thermal ellipsoids are drawn at the 30% probability level. Hydrogen atoms, except for the H(1) atom of (*Z*)-**1a**, are omitted for clarity. Selected bond distances (Å) and angles (deg) are as follows. (*E*)-**1a**: Pd–Br = 2.5324(8), Pd–P(1) = 2.3139(10), Pd–P(2) = 2.3121(10), Pd–C(1) = 2.007(2), C(1)–C(2) = 1.325(3), Br–Pd–P(1) = 94.15(2), Br–Pd–P(2) = 90.08(3), C(1)–Pd–P(1) = 88.32(7), C(1)–Pd–P(2) = 87.50(7), Pd–C(1)–C(2) = 128.85(18), C(1)–C(2)–C(3) = 123.4(2). (*Z*)-**1a**: Pd–Br = 2.5233(8), Pd–P(1) = 2.3187(12), Pd–P(2) = 2.3128(13), Pd–C(1) = 2.002(5), C(1)–C(2) = 1.341(7), Br–Pd–P(1) = 91.50(3), Br–Pd–P(2) = 95.55(3), C(1)–Pd–P(1) = 87.21(13), C(1)–Pd–P(2) = 85.75(13), Pd–C(1)–C(2) = 129.5(4), C(1)–C(2)–C(3) = 129.4(4).

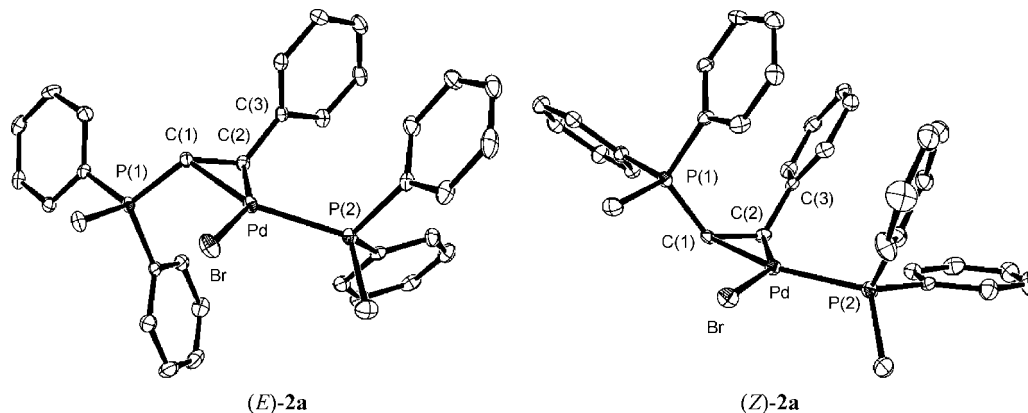


**Figure 2.** X-ray structures of (*E*)-**2a** and (*Z*)-**2a**. Thermal ellipsoids are drawn at the 30% probability level. Hydrogen atoms are omitted for clarity. Selected bond distances (Å) and angles (deg) are as follows. (*E*)-**2a**: Pd–Br = 2.5669(10), Pd–P(2) = 2.281(2), Pd–C(1) = 2.135(8), Pd–C(2) = 2.063(7), C(1)–P(1) = 1.758(8), C(1)–C(2) = 1.444(10), C(2)–C(3) = 1.491(10), Br–Pd–P(2) = 98.32(6), C(1)–Pd–C(2) = 40.2(3), Pd–C(1)–C(2) = 67.2(4), C(1)–Pd–Br = 115.1(2), C(2)–Pd–P(2) = 106.4(2), C(1)–C(2)–C(3) = 122.0(7), P(1)–C(1)–C(2) = 122.2(6). (*Z*)-**2a**: Pd–Br = 2.6201(10), Pd–P(2) = 2.2872(17), Pd–C(1) = 2.106(5), Pd–C(2) = 2.088(5), C(1)–P(1) = 1.754(5), C(1)–C(2) = 1.438(7), C(2)–C(3) = 1.494(7), Br–Pd–P(2) = 92.78(4), C(1)–Pd–C(2) = 40.1(2), Pd–C(1)–C(2) = 69.3(3), C(1)–Pd–Br = 111.83(15), C(2)–Pd–P(2) = 115.24(16), C(1)–C(2)–C(3) = 124.8(4), P(1)–C(1)–C(2) = 129.6(4).

that of (*Z*)-**2a** to (*Z*)-**1a** are operative under similar conditions, it seems likely that the observed tendencies mainly reflect the difference in thermodynamic stability between (*E*)- and (*Z*)-isomers of **1a** and **2a**. We therefore examined their structures by X-ray diffraction analysis and DFT calculations.

Figure 1 shows ORTEP drawings of (*E*)-**1a** and (*Z*)-**1a**. Both complexes have similar structures with comparable distances of Pd–C (2.00 Å), Pd–P (2.31 Å), and Pd–Br (2.53 Å) bonds. A notable difference between the isomers is found for the orientation of styryl ligands. The (*E*)-styryl ligand in (*E*)-**1a** is oriented away from the palladium center, successfully evading the steric congestion within the molecule. On the other hand, the phenyl group of the (*Z*)-styryl ligand in (*Z*)-**1a** is situated over the palladium center. Although the interatomic distance of Pd⋯H(1) (2.494 Å) is in the range of agostic interactions, a repulsive interaction between them should be considered, because the C(1)–C(2)–C(3) angle (129.4(4)°) is significantly enlarged as compared with that of (*E*)-**1a** (123.4(2)°).

Figure 2 shows the X-ray structures of (*E*)-**2a** and (*Z*)-**2a**. The C(1)–C(2) distances (1.444(10), 1.438(7) Å) are comparable to each other. The Pd, C(1), C(2), P(2), and Br atoms are coplanar in both molecules, as previously observed for related alkenylphosphonium complexes.<sup>5a,5b</sup> The Pd–C(1) bonds (2.135(8), 2.106(5) Å) are apparently longer than the Pd–C(2) bonds (2.063(7), 2.088(5) Å), reflecting the higher trans influence of PMePh<sub>2</sub> than Br.

A remarkable structural feature of (*Z*)-**2a** is the axial/axial arrangement of three phenyl groups of PhCH=CHP<sup>(1)</sup>MePh<sub>2</sub> and P<sup>(2)</sup>MePh<sub>2</sub> ligands. Since they are situated at 1,3-diaxial positions with one another, a great deal of steric repulsion should take place between them. This situation is in sharp contrast with (*E*)-**2a**, in which all substituents are accommodated with enough space. Actually, the P(1)–C(1)–C(2) angle of (*Z*)-**2a** (129.6(4)°) is apparently wider than that of (*E*)-**2a** (122.2(6)°).

**Table 3.** Relative Energies of **2a** to **1a** (kcal mol<sup>-1</sup>)<sup>a</sup>

solvent	( <i>E</i> )-isomers	( <i>Z</i> )-isomers
(in vacuo)	0.0	+4.3
C <sub>6</sub> H <sub>6</sub>	-2.3	+2.3
THF	-4.2	+0.4
CH <sub>2</sub> Cl <sub>2</sub>	-4.6	+1.0

<sup>a</sup> The values of  $E_{2a} - E_{1a}$ , estimated by DFT calculations.

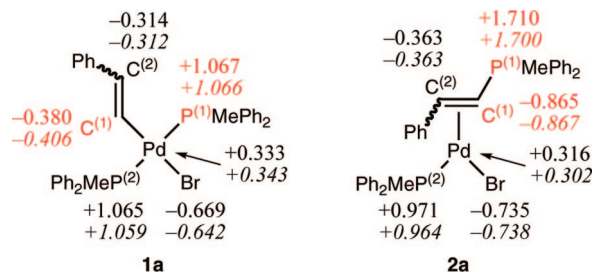


**Figure 3.** NBO charges on the core atoms of **1a** and **2a**. The values for (*E*)- and (*Z*)-isomers are given with roman and italic typefaces, respectively.

**DFT Calculations.** Table 3 lists the relative energies of **2a** to **1a**, estimated by DFT calculations. The geometry optimization of (*E*)- and (*Z*)-isomers of the complexes was carried out using B3LYP in conjunction with the LANL2DZ basis set and effective core potential for Pd and the 6-31G(d) basis set for other atoms, where a diffuse function was added for the Br atom. Solvent effects were incorporated by PCM single-point calculations on fully optimized geometries in vacuo. The optimized structures were in good accordance with the X-ray structures given in Figures 1 and 2.

The data in Table 3 clearly indicate that C–P reductive elimination of (*E*)-isomer [(*E*)-**1a** → (*E*)-**2a**] is an exothermic process, whereas that of (*Z*)-isomer [(*Z*)-**1a** → (*Z*)-**2a**] is endothermic (i.e., the reverse process is exothermic). Furthermore, reflecting the presence of the styrylphosphonium ligand with an ionic character, **2a** is more effectively stabilized than **1a** in polar solvents for both isomers. These tendencies are consistent with the experimental observations described above.

Figure 3 compares the charge distribution in **1a** and **2a**, evaluated by NBO analysis. The values written in roman and italic letters correspond to the atomic charges for (*E*)- and (*Z*)-isomers, respectively. The  $\eta^2$ -styrylphosphonium palladium complexes (**2**) are commonly depicted as zwitterionic species having positive and negative charges on the phosphorus and palladium atoms, respectively (see eqs 1 and 2). However, while the P(1) atom of **2a** is charged positively, the Pd atom is not

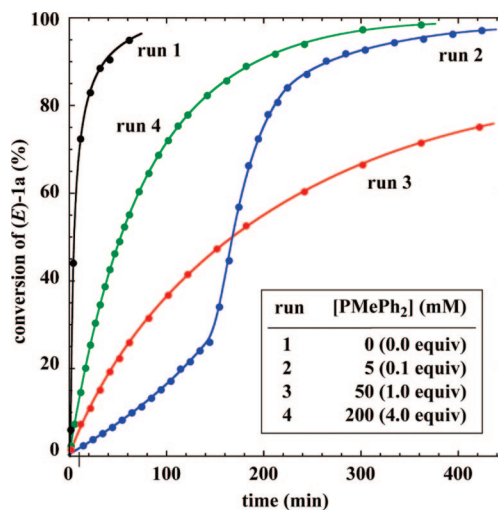


**Figure 4.** Time course of conversion of (*E*)-**1a** (50 mM) in CD<sub>2</sub>Cl<sub>2</sub> at 40 °C in the absence or presence of added PMePh<sub>2</sub>.

charged negatively in reality. The negative charge is distributed on the C(1), C(2), and Br atoms and most remarkably increased on the C(1) atom as compared with **1a**, showing the occurrence of strong  $\pi$ -back-donation from the palladium center to the  $\eta^2$ -styrylphosphonium ligand in **2a**.

**Mechanism of C–P Reductive Elimination.** As seen from Table 1 (runs 1, 2), the C–P reductive elimination of (*E*)-**1a** is strongly inhibited by added PMePh<sub>2</sub>, showing a reaction process involving predissociation of the PMePh<sub>2</sub> ligand (path (a) in Scheme 1). The three-coordinate intermediate **A** undergoes C–P reductive elimination to form **B**, which combines with PMePh<sub>2</sub> to afford (*E*)-**2a**. On the other hand, as described below, kinetic data revealed that the other reaction process involving prior association of PMePh<sub>2</sub> is operative in the presence of added PMePh<sub>2</sub> (path (b)).

Figure 4 shows the time course of conversion of (*E*)-**1a** (50 mM) in CD<sub>2</sub>Cl<sub>2</sub> at 40 °C, followed by <sup>1</sup>H NMR spectroscopy using 1,3,5-trimethoxybenzene as an internal standard. In the absence of free PMePh<sub>2</sub> (run 1), the PMe signal of (*E*)-**1a** at  $\delta$  2.07 rapidly decreased ( $t_{1/2}$  = ca. 5 min), to be replaced by the PMe signals of (*E*)-**2a** at  $\delta$  2.83 and 1.50. The reaction progress was effectively prevented by addition of a small amount of PMePh<sub>2</sub> (5 mM, 0.1 equiv/**1a**) to the system (run 2). In this case, however, the reaction dramatically accelerated from the middle stage, because the added PMePh<sub>2</sub> is consumed by trapping in the reductive elimination product as [Pd( $\eta^2$ -(*E*)-PhCH=CHPMePh<sub>2</sub>)(PMePh<sub>2</sub>)<sub>2</sub>]Br ((*E*)-**3a**). Indeed, in the <sup>1</sup>H

**Scheme 1.** Proposed Mechanisms for C–P Reductive Elimination of (*E*)-**1a**

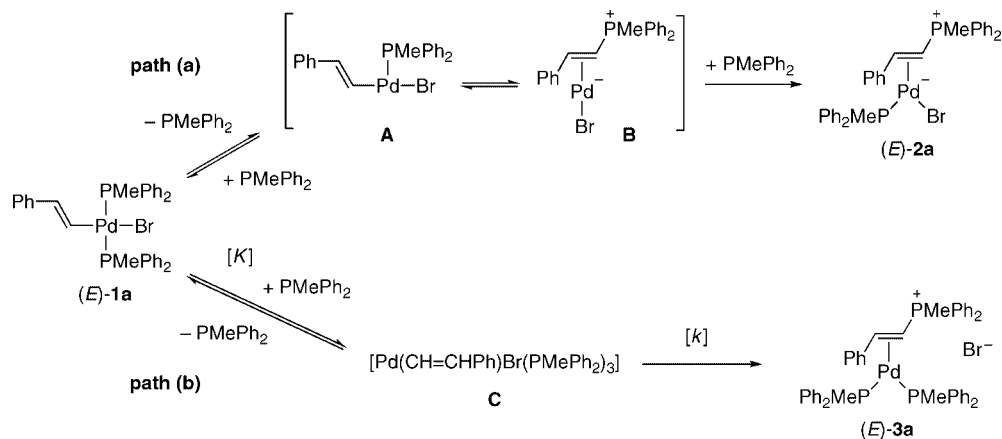


**Table 4.** Effects of Added  $\text{PMePh}_2$  on the First-Order Rate Constants for C–P Reductive Elimination of (*E*)-**1a**<sup>a</sup>

[ $\text{PMePh}_2$ ] (mM)	$10^4 k_{\text{obsd}}$ ( $\text{s}^{-1}$ )	data range (%) <sup>b</sup>
50	0.76(2)	19
64	0.87(1)	29
100	1.28(2)	38
200	2.14(1)	60

<sup>a</sup> [(*E*)-**1a**]<sub>0</sub> = 50 mM. All reactions were run at 40 °C in  $\text{CD}_2\text{Cl}_2$ .

<sup>b</sup> The upper range of the conversion of (*E*)-**1a**, taken into the first-order plot.

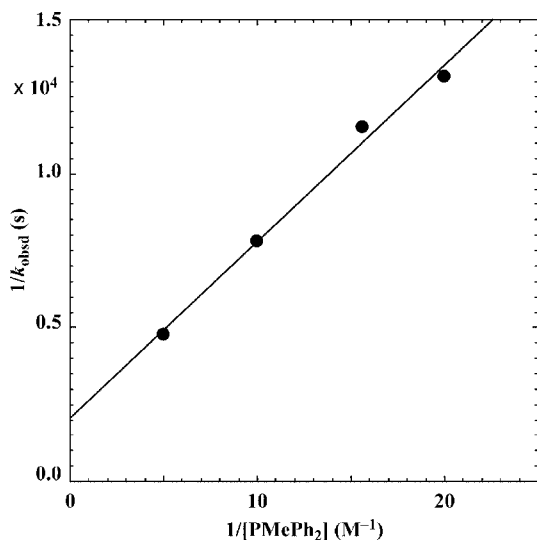


**Figure 5.** Plot of  $1/k_{\text{obsd}}$  against  $1/[\text{PMePh}_2]$  for the kinetic data in Table 4. The straight line is based on least-squares calculation:  $1/k_{\text{obsd}} = (5.7(4) \times 10^2 \text{ s M})/[\text{PMePh}_2] + (2.1(5) \times 10^3 \text{ s})$ .

NMR spectra, the  $\text{PMe}$  signal of (*E*)-**1a** was observed to be coalescent with that of  $\text{PMePh}_2$  until ca. 20% conversion of (*E*)-**1a**, but thereafter changed to a sharp triplet, showing the absence of free  $\text{PMePh}_2$  in the system.

Interestingly, the rate of C–P reductive elimination increased significantly with increasing amounts of added  $\text{PMePh}_2$  (runs 3 and 4). Thus, the reaction performed with 50 mM  $\text{PMePh}_2$  (run 3) was clearly faster than the initial stage of run 2 (5 mM) and accelerated further with 200 mM  $\text{PMePh}_2$  (run 4). Although the concentration of free  $\text{PMePh}_2$  gradually decreases with the formation of (*E*)-**3a**, the reactions obeyed a good first-order kinetics ( $r > 0.999$ ) up to 19% (run 3) and 60% (run 4) conversion of (*E*)-**1a**. Table 4 lists the rate constants ( $k_{\text{obsd}}$ ) thus estimated. The plot of  $1/k_{\text{obsd}}$  against  $1/[\text{PMePh}_2]$  exhibited a good linear correlation ( $r = 0.995$ , Figure 5).

These kinetic observations are consistent with the reaction process of path b in Scheme 1. Since (*E*)-**1a** undergoes rapid ligand exchange with free  $\text{PMePh}_2$  on an NMR time scale, the occurrence of a rapid equilibrium between (*E*)-**1a** and **C** is likely. Intermediate **C** then undergoes the rate-determining formation of (*E*)-**3a**. In this case, the reaction rate can be expressed by eq 3, where  $[\text{Pd-styryl}] = [(\text{E})\text{-1a}] + [\text{C}]$ ,  $K = [\text{C}]/[(\text{E})\text{-1a}][\text{PMePh}_2]$ , and  $k$  stands for the rate constant for the conversion of **C** to (*E*)-**3a**:

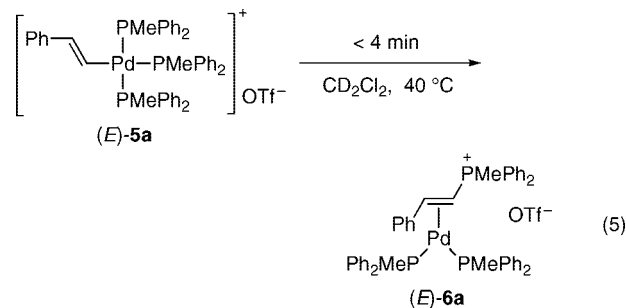
$$\frac{d[(\text{E})\text{-3a}]}{dt} = -\frac{d[\text{Pd-styryl}]}{dt} = \frac{kK[\text{PMePh}_2]}{1 + k[\text{PMePh}_2]}[\text{Pd-styryl}] \quad (3)$$

Consequently, the  $k_{\text{obsd}}$  values are correlated with the  $[\text{PMePh}_2]$  values by the following equation:

$$\frac{1}{k_{\text{obsd}}} = \frac{1}{kK[\text{PMePh}_2]} + \frac{1}{k} \quad (4)$$

Applying the slope and intercept values of Figure 5 to eq 4 results in the following rate and equilibrium constants:  $k = 4.8 \times 10^{-4} \text{ s}^{-1}$ ,  $K = 3.7 \text{ M}^{-1}$ .

There are two possible structures for intermediate **C**. One is a five-coordinate species, whereas the other is a four-coordinate ionic complex,  $[\text{Pd}\{\text{CH}=\text{CHPh}(\text{E})\}(\text{PMePh}_2)_3]^+\text{Br}^-$  ((*E*)-**4a**), generated by ligand displacement of  $\text{Br}$  in (*E*)-**1a** with  $\text{PMePh}_2$ . The C–P reductive elimination from the latter type intermediate has been postulated for catalytic conversion of alkenyl triflates and  $\text{PPh}_3$  to alkenylphosphonium triflates.<sup>5c,5d</sup> We therefore prepared  $[\text{Pd}\{\text{CH}=\text{CHPh}(\text{E})\}(\text{PMePh}_2)_3]^+\text{OTf}^-$  ((*E*)-**5a**) as a model of (*E*)-**4a** and examined its reactivity toward C–P reductive elimination (eq 5).



Treatment of (*E*)-**1a** (50 mM) with  $\text{AgOTf}$  (1 equiv) in  $\text{CD}_2\text{Cl}_2$  in the presence of  $\text{PMePh}_2$  (1 equiv) at  $-30$  °C for 1 h formed (*E*)-**5a** in 96% selectivity. The resulting (*E*)-**5a** was highly reactive toward C–P reductive elimination; the reaction was completed within a few minutes at 40 °C to give  $[\text{Pd}\{\eta^2\text{-}(\text{E})\text{-PhCH}=\text{CHPMePh}_2\}(\text{PMePh}_2)_2]\text{OTf}$  ((*E*)-**6a**) in 95% selectivity. No notable change in the reaction rate was observed in the presence of excess  $\text{PMePh}_2$  (4 equiv). Since the observed reactivity of (*E*)-**5a** ( $k > 5 \times 10^{-3} \text{ s}^{-1}$  at 40 °C) is at least 10 times higher than that of **C** ( $k = 4.8 \times 10^{-4} \text{ s}^{-1}$ ), it is convincing that **C** is not an ionic species like (*E*)-**5a**, but either a five-coordinate species or a tight ion pair of  $[\text{Pd}\{\text{CH}=\text{CHPh}(\text{E})\}(\text{PMePh}_2)_3]^+$  and  $\text{Br}^-$ . Complex **C** is then converted to (*E*)-**3a** by either a stepwise mechanism involving the metallophosphorane intermediate  $[\text{Pd}\{\text{P}(\text{CH}=\text{CHPh})\text{MePh}_2\}\text{Br}(\text{PMePh}_2)_2]$ <sup>13</sup> or a concerted mechanism with concurrent formation of the P–CH=CH and Pd–( $\eta^2$ -CH=CH) bonds.

## Conclusions

It has been evidenced that C–P reductive elimination of *trans*- $[\text{Pd}\{(\text{CH}=\text{CHPh})\text{Br}(\text{PMePh}_2)_2\}]$  (**1a**) is essentially a reverse process with C–P oxidative addition of styrylphosphonium complex  $[\text{Pd}\{\eta^2\text{-PhCH}=\text{CHPMePh}_2\}\text{Br}(\text{PMePh}_2)]$  (**2a**). The interconversion between **1a** and **2a** is markedly dependent on *E/Z* configurations of the styryl group and solvent polarity. The (*E*)-isomer of **1a** undergoes C–P reductive elimination easily in polar  $\text{CD}_2\text{Cl}_2$  to afford (*E*)-**2a** in high selectivity, whereas C–P oxidative addition of (*Z*)-**2a** giving (*Z*)-**1a** takes place favorably in nonpolar  $\text{C}_6\text{D}_6$ . These tendencies have been rationalized by X-ray structural analysis and DFT calculations

(13) A metallophosphorane intermediate has been proposed for F/Ph exchange of  $[\text{RhF}(\text{PPh}_3)_3]$  affording  $[\text{RhPh}(\text{PPh}_2)(\text{PPh}_3)_2]$ . Macgregor, S. A.; Roe, D. C.; Marshall, W. J.; Bloch, K. M.; Bakmutov, V. I.; Grushin, V. V. *J. Am. Chem. Soc.* **2005**, *127*, 15304–15321.

for **1a** and **2a**. Complex **2a**, bearing a styrylphosphonium ligand, is a significantly charged molecule, compared with **1a**, causing a strong solvent effect. Moreover, complex (*Z*)-**2a** is sterically unstable due to the occurrence of 1,3-diaxial interactions of phenyl groups within the molecule and thereby converted to (*Z*)-**1a** by C–P oxidative addition.

The reductive elimination from [PdR(R')L<sub>2</sub>]-type complexes has been known to proceed via any of three reaction processes: (a) dissociative path via a three-coordinate intermediate, (b) direct path, and (c) associative path with precoordination of an external L to give a [PdR(R')L<sub>3</sub>] intermediate.<sup>1a</sup> The reaction processes vary with hydrocarbyl ligands, and alkenyl complexes generally follow the direct path (b).<sup>14</sup> On the other hand, the present C–P reductive elimination from (*E*)-**1a** has been found to proceed via either the dissociative path (a) or the associative path (c), depending on the amount of free PMePh<sub>2</sub> in the system. In the absence of free PMePh<sub>2</sub>, the reaction invokes predissociation of one of the PMePh<sub>2</sub> ligands, giving a three-coordinate [Pd(CH=CHPh)Br(PMePh<sub>2</sub>)] intermediate, which undergoes C–P reductive elimination. This process is effectively suppressed by addition of PMePh<sub>2</sub> to the system, and an alternative process involving prior association of (*E*)-**1a** with PMePh<sub>2</sub> takes place. Comparison of the kinetic data with that of [Pd{CH=CHPh-(*E*)}(PMePh<sub>2</sub>)<sub>3</sub>]<sup>+</sup>OTf<sup>−</sup> (*E*)-**5a** has suggested the intermediacy of a five-coordinate species or a tight ion pair of [Pd{CH=CHPh-(*E*)}(PMePh<sub>2</sub>)<sub>3</sub>]<sup>+</sup> and Br<sup>−</sup>, rather than the four-coordinate ionic species like (*E*)-**5a**. Further mechanistic details, especially focused on the intermediate and transition state structures in the latter process (i.e., C → (*E*)-**3a** in Scheme 1), are now under investigation.

## Experimental Section

**General Considerations.** All manipulations were carried out under a nitrogen or argon atmosphere using standard Schlenk techniques. Nitrogen and argon gases were dried by passing through P<sub>2</sub>O<sub>5</sub> (Merck, SICAPENT). NMR spectra were recorded on a Bruker Avance 400 spectrometer (<sup>1</sup>H NMR 400.13 MHz, <sup>13</sup>C NMR 100.62 MHz, and <sup>31</sup>P NMR 161.97 MHz). Chemical shifts are reported in δ (ppm), referenced to the <sup>1</sup>H (residual protons) and <sup>13</sup>C signals of deuterated solvents or to the <sup>31</sup>P signal of an external 85% H<sub>3</sub>PO<sub>4</sub> standard. Elemental analysis was performed by the ICR Analytical Laboratory, Kyoto University. CD<sub>2</sub>Cl<sub>2</sub>, THF-*d*<sub>8</sub>, and C<sub>6</sub>D<sub>6</sub> were dried over CaH<sub>2</sub>, Na/Ph<sub>2</sub>CO, and LiAlH<sub>4</sub>, respectively, distilled, and stored over activated MS4A. The compounds *trans*-[Pd{CH=CHPh-(*E*)}Br(PMePh<sub>2</sub>)<sub>2</sub>] (*E*)-**1a**,<sup>11</sup> *trans*-[Pd{CH=CHPh-(*Z*)}Br(PMePh<sub>2</sub>)<sub>2</sub>] (*Z*)-**1a**,<sup>14a</sup> and [Pd{η<sup>2</sup>-(*E*)-PhCH=CHPMePh<sub>2</sub>}Br(PMePh<sub>2</sub>)<sub>2</sub>] (*E*)-**2a**<sup>11</sup> were prepared according to the literature. Other chemicals were purchased and used as received.

**Synthesis of *trans*-[Pd{CH=CHPh-(*E*)}Br(PPh<sub>3</sub>)<sub>2</sub>] (*E*)-**1b**.** To a heterogeneous solution of [Pd(η<sup>5</sup>-C<sub>5</sub>H<sub>5</sub>)(η<sup>3</sup>-C<sub>3</sub>H<sub>5</sub>)]<sup>15</sup> (106 mg, 0.500 mmol) and PPh<sub>3</sub> (275 mg, 1.05 mmol) in toluene (10 mL) was added (*E*)-styryl bromide<sup>16</sup> (1.83 g, 10.0 mmol) at 0 °C. The mixture was stirred at room temperature until homogeneous and then was allowed to stand at the same temperature, causing precipitation of pale yellow crystals of (*E*)-**1b**, which were collected by filtration, washed successively with Et<sub>2</sub>O, and dried under

vacuum (385 mg, 95% yield). The NMR data were identical to those reported.<sup>14a</sup> <sup>1</sup>H NMR (CD<sub>2</sub>Cl<sub>2</sub>): δ 7.70–7.63 and 7.43–7.30 (m, 30H in total), 6.98–6.87 (m, 3H), 6.40 (dt, <sup>3</sup>J<sub>HH</sub> = 15.7 Hz, <sup>3</sup>J<sub>HP</sub> = 9.7 Hz, 1H), 6.27 (d, <sup>3</sup>J<sub>HH</sub> = 6.8 Hz, 2H), 5.42 (dt, <sup>3</sup>J<sub>HH</sub> = 15.8 Hz, <sup>4</sup>J<sub>HP</sub> = 2.5 Hz, 1H). <sup>31</sup>P{<sup>1</sup>H} NMR (CD<sub>2</sub>Cl<sub>2</sub>): δ 24.5 (s).

**Synthesis of *trans*-[Pd{CH=CHPh-(*E*)}Br(PMe<sub>3</sub>)<sub>2</sub>] (*E*)-**1c**.** To a homogeneous solution of (η<sup>5</sup>-C<sub>5</sub>H<sub>5</sub>)(η<sup>3</sup>-C<sub>3</sub>H<sub>5</sub>)Pd<sup>15</sup> (106 mg, 0.500 mmol) in toluene (2.0 mL) was added PMe<sub>3</sub> (78.9 mg, 1.05 mmol) at 0 °C. The mixture was stirred for 10 min, and (*E*)-styryl bromide<sup>16</sup> (366 mg, 2.00 mmol) was added. The solution was stirred at room temperature for 4 h. Hexane (5 mL) was added with stirring at 0 °C. A white precipitate formed in the system was collected by filtration, washed successively with hexane (2 × 2 mL) and Et<sub>2</sub>O (2 × 2 mL), and dried under vacuum. The crude product was dissolved in a minimum amount of CH<sub>2</sub>Cl<sub>2</sub> (ca. 1 mL) at room temperature, layered with Et<sub>2</sub>O (ca. 5 mL), and allowed to stand at the same temperature to afford pale yellow crystals of the title compound (165 mg, 74% yield). Mp: 118–120 °C (dec). <sup>1</sup>H NMR (CD<sub>2</sub>Cl<sub>2</sub>): δ 7.33–7.21 and 7.12–7.07 (m, 6H in total), 6.43 (d, <sup>3</sup>J<sub>HH</sub> = 16.5 Hz, 1H), 1.38 (virtual triplet, *J* = 3.5 Hz, 18H). <sup>13</sup>C{<sup>1</sup>H} NMR (CD<sub>2</sub>Cl<sub>2</sub>): δ 145.6 (t, <sup>3</sup>J<sub>PC</sub> = 9 Hz), 140.4 (s), 134.3 (t, <sup>4</sup>J<sub>PC</sub> = 6 Hz), 129.0 (s), 125.9 (s), 125.2 (s), 14.6 (t, <sup>1</sup>J<sub>PC</sub> = 15 Hz). <sup>31</sup>P{<sup>1</sup>H} NMR (CD<sub>2</sub>Cl<sub>2</sub>): δ −17.9 (s). Anal. Calcd for C<sub>14</sub>H<sub>25</sub>BrP<sub>2</sub>D: C, 38.08; H, 5.71. Found: C, 37.96; H, 5.68.

**Synthesis of [Pd{(Z)-η<sup>2</sup>-PhCH=CHPMePh<sub>2</sub>}Br(PMePh<sub>2</sub>)] (*Z*)-**2a**.** (a) **Synthesis of (*Z*)-PhCH=CHPMePh<sub>2</sub> · Br.** A mixture of (*Z*)-P(CH=CHPh)Ph<sub>2</sub><sup>17</sup> (1.22 g, 4.25 mmol) and a 2 M solution of MeBr in THF (22 mL, 44 mmol) was stirred at room temperature. After 48 h, a white precipitate generated from the solution was collected by filtration, washed successively with Et<sub>2</sub>O, and dried under vacuum. Recrystallization of the crude product from a mixture of acetone and Et<sub>2</sub>O at −20 °C gave pale yellow crystals of the title compound (1.33 g, 82% yield). Mp: 130 °C. <sup>1</sup>H NMR (CDCl<sub>3</sub>): δ 8.30 (dd, <sup>2</sup>J<sub>HP</sub> = 45.4 Hz, <sup>3</sup>J<sub>HH</sub> = 13.2 Hz, 1H), 7.86–7.78, 7.73–7.67, and 7.63–7.57 (m, 10H in total), 7.22 (t, <sup>3</sup>J<sub>HH</sub> = 7.4 Hz, 1H), 7.13–7.05 (m, 3H), 7.01 (d, <sup>3</sup>J<sub>HH</sub> = 7.6 Hz, 2H), 2.74 (d, <sup>3</sup>J<sub>HP</sub> = 13.5 Hz, 3H). <sup>13</sup>C{<sup>1</sup>H} NMR (CDCl<sub>3</sub>): δ 158.0 (d, <sup>4</sup>J<sub>PC</sub> = 1 Hz), 134.6 (d, <sup>2</sup>J<sub>PC</sub> = 3 Hz), 133.5 (d, <sup>3</sup>J<sub>PC</sub> = 8 Hz), 132.6 (d, <sup>3</sup>J<sub>PC</sub> = 11 Hz), 130.4 (s), 130.3 (d, <sup>2</sup>J<sub>PC</sub> = 13 Hz), 128.5 (s), 128.4 (d, <sup>4</sup>J<sub>PC</sub> = 2 Hz), 120.2 (d, <sup>1</sup>J<sub>PC</sub> = 89 Hz), 110.0 (d, <sup>1</sup>J<sub>PC</sub> = 82 Hz), 12.2 (d, <sup>1</sup>J<sub>PC</sub> = 58 Hz). <sup>31</sup>P{<sup>1</sup>H} NMR (CDCl<sub>3</sub>): δ 12.9 (s). Anal. Calcd for C<sub>21</sub>H<sub>20</sub>BrP: C, 65.81; H, 5.26. Found: C, 65.67; H, 5.36.

(b) **Synthesis of (*Z*)-**2a**.** The complex Pd(dba)<sub>2</sub><sup>18</sup> (288 mg, 0.500 mmol) and (*Z*)-PhCH=CHPMePh<sub>2</sub> · Br (192 mg, 0.500 mmol) were dissolved in CH<sub>2</sub>Cl<sub>2</sub> (10 mL), and PMePh<sub>2</sub> (100 mg, 0.500 mmol) was added at room temperature. The mixture was stirred for 1 h and filtered through a Celite pad, and the filtrate was concentrated to dryness under reduced pressure. The residue was extracted three times with a mixed solvent of THF (2 mL) and Et<sub>2</sub>O, and the combined extract was concentrated to dryness to give a pale yellow solid of (*Z*)-**2a**. This product was purified three times by reprecipitation from CH<sub>2</sub>Cl<sub>2</sub>/Et<sub>2</sub>O (1/15 mL) at −78 °C and then by recrystallization from CH<sub>2</sub>Cl<sub>2</sub>/Et<sub>2</sub>O at −20 °C (162 mg, 47% yield). Mp: 117–119 °C (dec). <sup>1</sup>H NMR (CD<sub>2</sub>Cl<sub>2</sub>): δ 7.87–7.80, 7.71–7.64, 7.64–7.45, and 7.31–7.20 (m, 20H in total), 6.81 (d, <sup>3</sup>J<sub>HH</sub> = 7.0 Hz, 2H), 6.76 (t, <sup>3</sup>J<sub>HH</sub> = 7.3 Hz, 1H), 6.57 (t, <sup>3</sup>J<sub>HH</sub> = 7.7 Hz, 2H), 4.51 (ddd, <sup>2</sup>J<sub>HP</sub> = 27.3 Hz, <sup>3</sup>J<sub>HH</sub> = 10.7 Hz, <sup>3</sup>J<sub>HP</sub> = 5.3 Hz, 1H), 2.87 (ddd, <sup>3</sup>J<sub>HP</sub> = 11.9 Hz, <sup>3</sup>J<sub>HH</sub> = 10.7 Hz, <sup>3</sup>J<sub>HP</sub> = 8.1 Hz, 1H), 2.58 (d, <sup>2</sup>J<sub>HP</sub> = 13.6 Hz, 3H), 1.71 (d, <sup>2</sup>J<sub>HP</sub> = 6.1 Hz, 3H). <sup>13</sup>C{<sup>1</sup>H} NMR (CD<sub>2</sub>Cl<sub>2</sub>): δ 142.7 (dd, <sup>3</sup>J<sub>PC</sub> = 7 Hz, <sup>3</sup>J<sub>PC</sub> = 1 Hz), 139.0 (d, <sup>1</sup>J<sub>PC</sub> = 29 Hz), 138.8 (d, <sup>1</sup>J<sub>PC</sub> = 29 Hz), 133.9 (d, <sup>3</sup>J<sub>PC</sub> = 10 Hz), 133.2 (d, <sup>2</sup>J<sub>PC</sub> = 16 Hz), 133.1 (d, <sup>3</sup>J<sub>PC</sub> = 14 Hz), 133.0 (s), 132.9 (d, <sup>2</sup>J<sub>PC</sub> = 16 Hz), 131.0 (s), 131.0 (s), 129.6 (d, <sup>2</sup>J<sub>PC</sub> = 12 Hz),

(14) (a) Loar, M. K.; Stille, J. K. *J. Am. Chem. Soc.* **1981**, *103*, 4174–4181. (b) Brown, J. M.; Cooley, N. A. *Organometallics* **1990**, *9*, 353–359. (c) Calhorda, M. J.; Brown, J. M.; Cooley, N. A. *Organometallics* **1991**, *10*, 1431–1438. (d) Ozawa, F.; Tani, T.; Katayama, H. *Organometallics* **2005**, *24*, 2511–2515.

(15) Tatsuno, Y.; Yoshida, T.; Otsuka, S. *Inorg. Synth.* **1979**, *19*, 220–223.

(16) Dolby, L. J.; Wilkins, C.; Frey, T. G. *J. Org. Chem.* **1966**, *31*, 1110–1116.

(17) Taillefer, M.; Cristau, H. J.; Fruchier, A.; Vicente, V. *J. Organomet. Chem.* **2001**, *624*, 307–315.

(18) Ukai, T.; Kawamura, H.; Ishii, Y. *J. Organomet. Chem.* **1974**, *65*, 253–266.

Table 5. Crystal Data and Details of the Structure Determination for **1a** and **2a**

	( <i>E</i> )- <b>1a</b>	( <i>Z</i> )- <b>1a</b>	( <i>E</i> )- <b>2a</b>	( <i>Z</i> )- <b>2a</b>
formula	C <sub>34</sub> H <sub>33</sub> BrP <sub>2</sub> Pd			
fw	689.85	689.85	689.85	689.85
cryst size (mm)	0.40 × 0.20 × 0.10	0.28 × 0.20 × 0.08	0.40 × 0.19 × 0.18	0.08 × 0.05 × 0.01
cryst syst	triclinic	monoclinic	monoclinic	triclinic
<i>a</i> (Å)	7.263(3)	19.196(6)	9.7501(19)	9.097(3)
<i>b</i> (Å)	10.521(4)	16.509(5)	25.206(5)	11.925(4)
<i>c</i> (Å)	20.015(8)	20.194(7)	12.916(2)	14.187(5)
$\alpha$ (deg)	85.512(12)	90	90	77.931(12)
$\beta$ (deg)	86.222(12)	111.543(4)	109.107(3)	84.226(13)
$\gamma$ (deg)	79.225(11)	90	90	80.528(12)
<i>V</i> (Å <sup>3</sup> )	1495.9(10)	5952(3)	2999.4(10)	1480.9(9)
<i>d</i> <sub>calc</sub> (g cm <sup>-3</sup> )	1.532	1.540	1.523	1.547
space group	<i>P</i> $\bar{1}$ (#2)	<i>P</i> 2 <sub>1</sub> / <i>c</i> (#14)	<i>Cc</i> (#9)	<i>P</i> $\bar{1}$ (#2)
<i>Z</i>	2	8	4	2
$\mu$ (mm <sup>-1</sup> )	2.085	2.095	2.079	2.106
transmn factor	0.4894–0.8186	0.5915–0.8503	0.5936–0.7060	0.6781–0.6781
absorp corr	numerical	numerical	numerical	empirical
$\theta$ range (deg)	3.09–27.48	3.06–27.48	3.23–27.48	3.08–27.48
no. of reflns collected	12 140	46 439	12 140	12 141
no. of unique reflns	6577 ( <i>R</i> <sub>int</sub> = 0.0340)	13 534 ( <i>R</i> <sub>int</sub> = 0.0642)	5855 ( <i>R</i> <sub>int</sub> = 0.0267)	6521 ( <i>R</i> <sub>int</sub> = 0.0541)
no. of reflns with <i>I</i> > 2 $\sigma$ ( <i>I</i> )	5758	10 727	4546	4103
no. of variables (restraints)	345 (0)	693 (0)	338 (2)	345 (0)
GOF on <i>F</i> <sup>2</sup>	1.058	0.930	1.048	1.059
final <i>R</i> indices ( <i>I</i> > 2 $\sigma$ ( <i>I</i> ))	<i>R</i> <sub>1</sub> = 0.0297, <i>wR</i> <sub>2</sub> = 0.0726	<i>R</i> <sub>1</sub> = 0.0498, <i>wR</i> <sub>2</sub> = 0.1305	<i>R</i> <sub>1</sub> = 0.0496, <i>wR</i> <sub>2</sub> = 0.1335	<i>R</i> <sub>1</sub> = 0.0545, <i>wR</i> <sub>2</sub> = 0.0898
<i>R</i> indices (all data)	<i>R</i> <sub>1</sub> = 0.0360, <i>wR</i> <sub>2</sub> = 0.0761	<i>R</i> <sub>1</sub> = 0.0732, <i>wR</i> <sub>2</sub> = 0.1496	<i>R</i> <sub>1</sub> = 0.0586, <i>wR</i> <sub>2</sub> = 0.1374	<i>R</i> <sub>1</sub> = 0.1015, <i>wR</i> <sub>2</sub> = 0.1121
max. and min. peak (e Å <sup>-3</sup> )	0.806, –0.823	1.158, –0.515	0.984, –0.900	1.099, –0.865

129.3 (d, <sup>5</sup>*J*<sub>PC</sub> = 1 Hz), 129.1 (s), 129.1 (d, <sup>2</sup>*J*<sub>PC</sub> = 12 Hz), 128.4 (d, <sup>3</sup>*J*<sub>PC</sub> = 9 Hz), 128.4 (d, <sup>3</sup>*J*<sub>PC</sub> = 9 Hz), 127.3 (s), 126.9 (dd, <sup>1</sup>*J*<sub>PC</sub> = 80 Hz, <sup>4</sup>*J*<sub>PC</sub> = 7 Hz), 125.9 (dd, <sup>1</sup>*J*<sub>PC</sub> = 84 Hz, <sup>4</sup>*J*<sub>PC</sub> = 4.3 Hz), 125.5 (s), 60.9 (s), 32.3 (dd, <sup>1</sup>*J*<sub>PC</sub> = 78 Hz, <sup>2</sup>*J*<sub>PC</sub> = 38 Hz), 16.6 (dd, <sup>1</sup>*J*<sub>PC</sub> = 66 Hz, <sup>4</sup>*J*<sub>PC</sub> = 2 Hz), 15.2 (d, <sup>1</sup>*J*<sub>PC</sub> = 15 Hz). <sup>31</sup>P{<sup>1</sup>H} NMR (CD<sub>2</sub>Cl<sub>2</sub>):  $\delta$  17.5 (d, <sup>3</sup>*J*<sub>PP</sub> = 9 Hz), 6.1 (d, <sup>3</sup>*J*<sub>PP</sub> = 9 Hz). Anal. Calcd for C<sub>34</sub>H<sub>33</sub>BrPPd: C, 59.19; H, 4.82. Found: C, 58.75; H, 4.92.

**C–P Reductive Elimination and Oxidative Addition.** A typical procedure is as follows. (*E*)-**1a** (20.7 mg, 0.030 mmol) and 1,3,5-trimethoxybenzene (2.5 mg, 0.015 mmol; internal standard) were placed in an NMR sample tube and dissolved in CD<sub>2</sub>Cl<sub>2</sub> (total 0.6 mL) at room temperature under an argon atmosphere. The sample tube was placed in an NMR sample probe controlled to 40.0 ± 0.1 °C. The reaction was examined at intervals by <sup>1</sup>H NMR spectroscopy using the following marker signals: (*E*)-**1a** ( $\delta$  2.07, PMe), (*E*)-**2a** ( $\delta$  2.83, PMe), (*E*)-**3a** ( $\delta$  1.18, PMe), *trans*-[PdBr<sub>2</sub>(PMePh<sub>2</sub>)<sub>2</sub>] ( $\delta$  2.24, PMe).

The complex [Pd{ $\eta^2$ -(*E*)-PhCH=CHPMePh<sub>2</sub>}(PMePh<sub>2</sub>)<sub>2</sub>]Br ((*E*)-**3a**) was independently prepared from (*E*)-**2a** and PMePh<sub>2</sub> (1 equiv) in CD<sub>2</sub>Cl<sub>2</sub> and characterized by NMR spectroscopy. <sup>1</sup>H NMR (CD<sub>2</sub>Cl<sub>2</sub>):  $\delta$  7.81–7.21, 7.20–7.05, 6.73–6.67, and 6.67–6.55 (m, 35H in total), 3.74–3.58 (m, 2H), 1.98 (d, <sup>2</sup>*J*<sub>HP</sub> = 13.1 Hz, 3H), 1.59 (d, <sup>2</sup>*J*<sub>HP</sub> = 4.9 Hz, 3H), 1.12 (d, <sup>2</sup>*J*<sub>HP</sub> = 6.1 Hz, 3H). <sup>31</sup>P{<sup>1</sup>H} NMR (CD<sub>2</sub>Cl<sub>2</sub>):  $\delta$  21.4 (br), 4.5 (br), 4.2 (br). The formation of (*E*)-**3a** took place instantly at room temperature, as already documented for (*E*)-**3b**.<sup>12</sup>

**Synthesis and C–P Reductive Elimination of [Pd{CH=CHPh-(*E*)}(PMePh<sub>2</sub>)<sub>3</sub>]OTf ((*E*)-**5a**).** Complex (*E*)-**1a** (27.6 mg, 0.040 mmol), PMePh<sub>2</sub> (8.0 mg, 0.040 mmol), and 1,3,5-trimethoxybenzene (3.4 mg, 0.020 mmol; internal standard) were dissolved in CD<sub>2</sub>Cl<sub>2</sub> (0.75 mL), and AgOTf (10.3 mg, 0.400 mmol) was added at –30 °C. The solution was stirred at this temperature for 1 h to precipitate an off-white powder of AgBr. The orange supernatant was transferred by cannulation to an NMR sample tube and analyzed by <sup>1</sup>H NMR spectroscopy at –30 °C, showing the formation of (*E*)-**5a** (96%) and a small amount of [Pd{ $\eta^2$ -(*E*)-PhCH=CHPMePh<sub>2</sub>}(PMePh<sub>2</sub>)<sub>2</sub>]OTf ((*E*)-**6a**) (3%). At 40 °C, (*E*)-**5a** was converted to (*E*)-**6a** within 4 min in 95% selectivity. Since (*E*)-**5a** was thermally too unstable to be isolated, its characterization was carried out by NMR spectroscopy.

(*E*)-**5a**. <sup>1</sup>H NMR (CD<sub>2</sub>Cl<sub>2</sub>, –30 °C):  $\delta$  7.46–7.15 and 7.02–6.92 (m, 33H in total), 6.29 (d, <sup>3</sup>*J*<sub>HH</sub> = 7.3 Hz, 2H), 6.14 (tdd, <sup>3</sup>*J*<sub>HP</sub> = 20.6 Hz, <sup>3</sup>*J*<sub>HH</sub> = 16.6 Hz, <sup>3</sup>*J*<sub>HP</sub> = 10.5 Hz, 1H), 5.72 (dd, <sup>3</sup>*J*<sub>HH</sub> = 16.6 Hz, <sup>4</sup>*J*<sub>HP</sub> = 10.2 Hz, 1H), 1.66 (virtual triplet, *J* = 3.1 Hz, 6H), 1.30 (t, <sup>2</sup>*J*<sub>HP</sub> = 7.2 Hz, 3H). <sup>31</sup>P{<sup>1</sup>H} NMR (CD<sub>2</sub>Cl<sub>2</sub>, –30 °C):  $\delta$  7.9 (d, <sup>2</sup>*J*<sub>PP</sub> = 35 Hz), –0.53 (t, <sup>2</sup>*J*<sub>PP</sub> = 35 Hz).

(*E*)-**6a**. <sup>1</sup>H NMR (CD<sub>2</sub>Cl<sub>2</sub>):  $\delta$  7.82–7.76, 7.70–7.56, 7.52–7.23, 7.16–7.10, 6.72–6.66, and 6.66–6.56 (m, 35H in total), 3.72–3.51 (m, 2H), 1.85 (d, <sup>2</sup>*J*<sub>HP</sub> = 13.1 Hz, 3H), 1.57 (d, <sup>2</sup>*J*<sub>HP</sub> = 5.3 Hz, 3H), 1.12 (d, <sup>2</sup>*J*<sub>HP</sub> = 6.1 Hz, 3H). <sup>13</sup>C{<sup>1</sup>H} NMR (CD<sub>2</sub>Cl<sub>2</sub>):  $\delta$  142.1 (dd, <sup>3</sup>*J*<sub>PC</sub> = 12 Hz, <sup>3</sup>*J*<sub>PC</sub> = 7 Hz), 138.5 (dd, <sup>1</sup>*J*<sub>PC</sub> = 29 Hz, <sup>3</sup>*J*<sub>PC</sub> = 3 Hz), 137.5 (dd, <sup>1</sup>*J*<sub>PC</sub> = 31 Hz, <sup>3</sup>*J*<sub>PC</sub> = 3 Hz), 136.8 (dd, <sup>1</sup>*J*<sub>PC</sub> = 30 Hz, <sup>3</sup>*J*<sub>PC</sub> = 1 Hz), 134.5 (d, <sup>4</sup>*J*<sub>PC</sub> = 3 Hz), 134.4 (d, <sup>4</sup>*J*<sub>PC</sub> = 3 Hz), 134.4 (dd, <sup>1</sup>*J*<sub>PC</sub> = 31 Hz, <sup>3</sup>*J*<sub>PC</sub> = 2 Hz), 133.0 (d, <sup>3</sup>*J*<sub>PC</sub> = 10 Hz), 132.6 (d, <sup>3</sup>*J*<sub>PC</sub> = 10 Hz), 132.6 (d, <sup>2</sup>*J*<sub>PC</sub> = 14 Hz), 132.3 (d, <sup>2</sup>*J*<sub>PC</sub> = 14 Hz), 131.7 (d, <sup>2</sup>*J*<sub>PC</sub> = 14 Hz), 131.2 (d, <sup>2</sup>*J*<sub>PC</sub> = 13 Hz), 130.7 (d, <sup>4</sup>*J*<sub>PC</sub> = 1 Hz), 130.3 (d, <sup>2</sup>*J*<sub>PC</sub> = 12 Hz), 130.2 (s), 130.1 (d, <sup>2</sup>*J*<sub>PC</sub> = 12 Hz), 129.6 (d, <sup>4</sup>*J*<sub>PC</sub> = 1 Hz), 129.4 (d, <sup>3</sup>*J*<sub>PC</sub> = 9 Hz), 129.4 (d, <sup>3</sup>*J*<sub>PC</sub> = 9 Hz), 129.2 (m), 128.8 (d, <sup>3</sup>*J*<sub>PC</sub> = 9 Hz), 128.7 (d, <sup>3</sup>*J*<sub>PC</sub> = 9 Hz), 126.2 (m), 125.2 (m), 124.6 (dd, <sup>1</sup>*J*<sub>PC</sub> = 89 Hz, <sup>3</sup>*J*<sub>PC</sub> = 2 Hz), 124.4 (dd, <sup>1</sup>*J*<sub>PC</sub> = 83 Hz, <sup>3</sup>*J*<sub>PC</sub> = 5 Hz), 121.6 (q, <sup>1</sup>*J*<sub>FC</sub> = 321 Hz), 65.7 (dd, <sup>2</sup>*J*<sub>PC</sub> = 31 Hz, <sup>2</sup>*J*<sub>PC</sub> = 5 Hz), 34.0 (ddd, <sup>1</sup>*J*<sub>PC</sub> = 79 Hz, <sup>2</sup>*J*<sub>PC</sub> = 32 Hz, <sup>2</sup>*J*<sub>PC</sub> = 7 Hz), 15.1 (d, <sup>1</sup>*J*<sub>PC</sub> = 19 Hz), 13.0 (d, <sup>1</sup>*J*<sub>PC</sub> = 20 Hz), 11.6 (d, <sup>1</sup>*J*<sub>PC</sub> = 64 Hz). <sup>31</sup>P{<sup>1</sup>H} NMR (CD<sub>2</sub>Cl<sub>2</sub>):  $\delta$  21.3 (d, <sup>2</sup>*J*<sub>PP</sub> = 12 Hz), 4.4 (s), 4.1 (d, <sup>2</sup>*J*<sub>PP</sub> = 12 Hz).

**X-ray Structural Analysis.** Single crystals of (*E*)-**1a**, (*Z*)-**1a**, (*E*)-**2a**, and (*Z*)-**2a** were grown by slow diffusion of Et<sub>2</sub>O into CH<sub>2</sub>Cl<sub>2</sub> solutions at –20 °C ((*E*)-**1a**, (*E*)-**2a**, (*Z*)-**2a**) and –30 °C ((*Z*)-**1a**), respectively. The intensity data were collected on a Rigaku Mercury CCD diffractometer with graphite-monochromated Mo K $\alpha$  radiation ( $\lambda$  = 0.71070 Å). The intensity data were collected at 173 K and corrected for Lorentz and polarization effects and for absorption. The structures were solved by heavy atom Patterson methods (PATTY), expanded using Fourier techniques (DIRDIF99),<sup>19</sup> and refined on *F*<sup>2</sup> for all reflections (SHELXL-97).<sup>20</sup> All non-hydrogen atoms were refined anisotropically. The H(1)

(19) Beurskens, P. T.; Beurskens, G.; de Gelder, R.; García-Grana, S.; Gould, R. O.; Israel, R.; Smits, J. M. M. *The DIRDIF99 Program System*; University of Nijmegen: The Netherlands, 1999.

(20) Sheldrick, G. M. *SHELXL-97*; University of Gottingen: Germany, 1997.

atom of (Z)-**1a** was located from a differential Fourier map and refined isotropically. The other hydrogen atoms were placed using AFIX instructions. Crystal data and details of data collection and refinement are summarized in Table 5.

**Computational Details.** All calculations were performed using the B3LYP level of density functional theory.<sup>21</sup> The Pd atom was described using the LANL2DZ basis set including a double- $\zeta$  basis set with the Hay and Wadt effective core potential (ECP).<sup>22</sup>

---

(21) (a) Becke, A. D. *Phys. Rev. A* **1988**, *38*, 3098–3100. (b) Lee, C.; Yang, W.; Parr, R. G. *Phys. Rev. B* **1988**, *37*, 785–789. (c) Becke, A. D. *J. Chem. Phys.* **1993**, *98*, 5648–5652.

(22) Wadt, W. R.; Hay, P. J. *J. Chem. Phys.* **1985**, *82*, 284–298.

(23) Francel, M. M.; Pietro, W. J.; Hehre, W. J.; Binkley, J. S.; Gordon, M. S.; DeFrees, D. J.; Pople, J. A. *J. Chem. Phys.* **1982**, *77*, 3654–3665.

(24) Frisch, M. J.; Trucks, G. W.; Schlegel, H. B.; Scuseria, G. E.; Robb, M. A.; Cheeseman, J. R.; Montgomery, J. A., Jr.; Vreven, T.; Kudin, K. N.; Burant, J. C.; Millam, J. M.; Iyengar, S. S.; Tomasi, J.; Barone, V.; Mennucci, B.; Cossi, M.; Scalmani, G.; Rega, N.; Petersson, G. A.; Nakatsuji, H.; Hada, M.; Ehara, M.; Toyota, K.; Fukuda, R.; Hasegawa, J.; Ishida, M.; Nakajima, T.; Honda, Y.; Kitao, O.; Nakai, H.; Klene, M.; Li, X.; Knox, J. E.; Hratchian, H. P.; Cross, J. B.; Adamo, C.; Jaramillo, J.; Gomperts, R.; Stratmann, R. E.; Yazyev, O.; Austin, A. J.; Cammi, R.; Pomelli, C.; Ochterski, J. W.; Ayala, P. Y.; Morokuma, K.; Voth, G. A.; Salvador, P.; Dannenberg, J. J.; Zakrzewski, V. G.; Dapprich, S.; Daniels, A. D.; Strain, M. C.; Farkas, O.; Malick, D. K.; Rabuck, A. D.; Raghavachari, K.; Foresman, J. B.; Ortiz, J. V.; Cui, Q.; Baboul, A. G.; Clifford, S.; Cioslowski, J.; Stefanov, B. B.; Liu, G.; Liashenko, A.; Piskorz, P.; Komaromi, I.; Martin, R. L.; Fox, D. J.; Keith, T.; Al-Laham, M. A.; Peng, C. Y.; Nanayakkara, A.; Challacombe, M.; Gill, P. M. W.; Johnson, B.; Chen, W.; Wong, M. W.; Gonzalez, C.; Pople, J. A. *Gaussian 03*; Gaussian, Inc.: Pittsburgh, PA, 2004.

The 6-31G(d) basis set was used for other atoms.<sup>23</sup> A diffuse function was added for Br atoms. Frequency calculations were carried out to identify all the stationary states as minima (zero imaginary frequencies). All calculations in this study have been performed without any symmetry constraints using Gaussian 03.<sup>24</sup> The solvent effect was taken into account through single-point calculations at each optimized geometry in vacuo using the polarized continuum model (PCM) at 298.15 K.<sup>25</sup> The partial atomic charges were calculated on the basis of natural bond orbital (NBO) analyses.<sup>26</sup>

**Acknowledgment.** This work was supported by Grants-in-Aid for Scientific Research (Nos. 18064010 and 20350049) from the Ministry of Education, Culture, Sports, Science, and Technology, Japan.

**Supporting Information Available:** Tables with Cartesian coordinates of the optimized structures; crystallographic data in CIF format. This material is available free of charge via the Internet at <http://pubs.acs.org>.

OM801207K

---

(25) (a) Miertus, S.; Scrocco, E.; Tomasi, J. *J. Chem. Phys.* **1981**, *55*, 117–119. (b) Tomasi, J.; Persico, M. *Chem. Rev.* **1994**, *94*, 2027–2094. (c) Tomasi, J.; Cammi, R. *J. Comput. Chem.* **1995**, *16*, 1449–1458.

(26) Glendening, E. D.; Read, A. E.; Carpenter, J. E.; Weinhold, F. *NBO (version 3.1)*; Gaussian, Inc.: Pittsburgh, PA, 2004.